# Effect of foveal tritanopia on reaction times to chromatic stimuli

N.R.A. PARRY,[1] S. PLAINIS,[2] I.J. MURRAY,[3] AND D.J. McKEEFRY[4]

[1]Vision Science Centre, Manchester Royal Eye Hospital, UK
[2]VEIC, School of Medicine, University of Crete, Greece
[3]Visual Sciences Lab, Optometry & Neuroscience, UMIST, Manchester, UK
[4]Optometry, University of Bradford, UK

## Abstract

To investigate the effect of foveal inhomogeneities on sensitivity to chromatic stimuli, we measured simple reaction times (RTs) and detection thresholds to temporally and spatially blurred isoluminant stimuli at retinal eccentricities from 0 deg to 8 deg. Three color-normal subjects participated. Contrast gain was derived from the slope of the RT versus contrast function. With a Gaussian spatial distribution (S.D. = 0.5 deg) and modulation between white (CIE $x, y, L$ = 0.31, 0.316, 12.5 cd.m$^{-2}$) and blue (MBDKL 90 deg), gain was maximal at about 2-deg eccentricity and declined by approximately 1 log unit towards the center and the periphery. The red (0 deg) and green (180 deg) cardinal axes showed maximum gain in the center, whilst the yellow (270 deg) data were intermediate. Although the spatial extent of the Gaussian spot was much larger than the S-cone free zone, we wished to determine whether foveal tritanopia was responsible for the marked drop in sensitivity to the 90-deg stimulus. To align the color vector along a tritan line, we used a smaller disk (0.3 deg) with a blurred edge and measured detection threshold, rotating the vector until minimum central sensitivity was obtained. Other workers have used transient tritanopia or minimally distinct border to similar effect. By repeating this at different locations in color space, a group of vectors were obtained. These converged near to the S-cone co-punctal point, evidence that they lay along tritan confusion lines. These threshold findings were then confirmed using the RT-derived contrast gain function. The tritan vectors were less pronounced as stimulus size increased. With the vector optimized to produce foveal tritanopia, the RT gain versus eccentricity functions for the 90-deg and 270-deg stimuli both fell markedly in the center and periphery, and sensitivity peaked at about 3-deg eccentricity. There are some similarities between these findings and the underlying photoreceptor distributions. As a result, there is a greater difference in gain between red–green and blue–yellow systems in the center than in the near periphery. We conclude that the RT versus contrast function is a sensitive index of foveal opponency.

**Keywords:** Reaction time, Color opponency, Foveal tritanopia, Contrast threshold, Contrast gain

## Introduction

We have recently shown that the extent of variation of the simple reaction time (RT) with chromatic axis depends on the contrast metric used (McKeefry et al., 2003). The use of equal visibility suprathreshold contrast levels minimizes, but does not eliminate altogether, the apparent faster RTs to red–green compared with blue–yellow stimuli. These differences remained despite careful control of the spatial and temporal profiles of the stimuli as a means of reducing the contributions of luminance/non-color opponent mechanisms. Yet, in another study, where the authors were equally as careful to minimize the involvement of non-chromatic mechanisms, RT was found to remain constant as a function of stimulus chromaticity (Smithson & Mollon, 2001). Experimental

differences may prove to be the source of these discrepancies. In particular, Smithson and Mollon employed paracentral stimuli, as opposed to the central stimuli used by McKeefry et al.

Perhaps one of the most important differences between these stimulus regimes is the relative density of the various cone classes. The aim of the present study was to determine the influence of stimulus retinal eccentricity and the role played by retinal photoreceptor inhomogeneities. Anatomical studies of the human retina have revealed that L- and M-cones reach their maximum density centrally, whereas S-cones peak at around 1-deg eccentricity (Curcio et al., 1990, 1991). In McKeefry et al.'s study, a very small centrally fixated stimulus was employed, and thus foveal tritanopia (Williams et al., 1981) may explain the superiority of RT responses to red–green stimuli.

The RT itself is strongly dependent on stimulus contrast, but our focus in the present study is on contrast gain derived from the RT rather than on individual RTs which are frequently regarded as a measure of temporal delay. The RT versus contrast function can

provide a direct measure of contrast gain and is thus very helpful in obtaining an understanding of suprathreshold contrast processing. It is well known that contrast gain is closely related to threshold; a mechanism exhibiting low contrast thresholds must have high contrast gain and *vice versa*. This principle is evident in RT versus 1/contrast (1/C) functions (Murray & Plainis, 2003) and can be utilized to investigate the processing of chromatic information. There is a wide range of stimulus conditions in which the RT is a linear function of the reciprocal of contrast, the slope providing a direct measure of contrast gain (Plainis & Murray, 2000). This approach was used in the McKeefry et al. (2003) study to show that the gain of the blue–yellow mechanism is considerably less than that of red–green.

Here a rapid technique for determining the RT gain function is described. This new method is used to study the effect of retinal photoreceptor distribution on contrast gain in different regions of color space.

## Materials and methods

### Stimuli

Colored spots on a white background were presented on a Sony GDM F-520 CRT display by means of a VSG2/3 stimulus generator card (Cambridge Research Systems Ltd, Rochester, UK) in a Pentium computer. Stimuli were defined as contrast vectors oriented in CIE 1931 color space to produce modulation along MBDKL cardinal axes 0, 90, 180, and 270 deg (MacLeod & Boynton, 1979; Derrington et al., 1984). These axes are nominally designed for maximum activation of the two color opponent axes [0 deg = $+L-M$, 90 deg = $+S-(L+M)$, 180 deg = $-L+M$, 270 deg = $-S+(L+M)$]. The background was illuminant C ($x, y, L = 0.31, 0.316, 12.5$ cd.m$^{-2}$), and the $x, y$ CIE 1931 chromaticity coordinates of the four principal vectors were 0 deg: 0.3819, 0.2826; 90 deg: 0.2724, 0.2280; 180 deg: 0.2197, 0.3584; and 270 deg: 0.3926, 0.5092. The vectors could be shifted in small steps around color space. This was usually achieved by fixing the white point and rotating the colored end of the vector.

For most of these experiments, two radially symmetrical spatial configurations were used: either a Gaussian spot with a S.D. of 0.5 deg, or a blurred disk with a 0.3-deg-diameter flat top and a raised consinusoidal skirt of 0.6-deg diameter. Some experiments were conducted with larger disks (0.6 deg with a 1.2-deg skirt and 0.9 deg with a 1.8-deg skirt). For reaction timing, the stimuli were temporally modulated with a raised cosinusoidal attack of 190 ms, 190 ms at maximum contrast, and a raised cosinusoidal decay of 190 ms. Stimuli were viewed monocularly at a distance of 1 m, and a black fixation spot with a diameter of 0.06 deg was provided. The background subtended 17.4 deg wide by 14.1 deg high. Mild head restraint was employed.

The gamma functions for the red, green, and blue guns were calibrated with a PR-650 spectroradiometer (Photoresearch, Chatsworth, CA). By concentrating the calibration procedure around the gun luminances employed in this study, we were able to achieve an accuracy of 0.002 in CIE $x, y$ chromaticity coordinates, and 0.01 cd.m$^{-2}$.

### Psychophysics

For each condition, isoluminance was determined using heterochromatic flicker photometry. The stimulus was flickered on and off at 10 Hz on a constant white background (12.5 cd.m$^{-2}$) while the subject adjusted the luminance of the (colored) end point of the vector in steps of 0.01 cd.m$^{-2}$. Isoluminance was defined as the point at which the subject perceived minimum flicker.

Threshold was determined using a binary-search staircase with a contrast resolution of 1 dB (0.05 log units). Initially, the stimulus (1-Hz sinusoidal modulation) was presented with a contrast of 16 dB. If seen, contrast was decreased by 16 dB. If not, it was increased by 16 dB. Successive increments were halved until the increment was less than 1 dB, and the resultant contrast taken as threshold. Thus threshold could be determined in six steps. If on the second presentation the stimulus was not seen at 0 dB, the procedure was abandoned. If it was still seen at 32 dB, the next increment was doubled, and successive increments halved. This added two steps to the procedure. For most of the experiments described here, the average of four threshold settings was taken.

### Reaction timing

In a single run, 64 stimuli were presented. The first was at full contrast (i.e. 100% of the vector length), and the last was close to threshold. The intervening stimuli were presented in equal steps between first and last values on a 1/C scale. Each stimulus was presented with the raised cosinusoidal flat-topped temporal function described above. The subject pressed a lever switch (CB3 box, Cambridge Research Systems, Rochester, UK) as soon as the stimulus was seen. The next stimulus was presented after an equal-likelihood random interval of between 1000 and 3000 ms. If no response was made, the interstimulus interval (ISI) was 5000 ms. The VSG card contains a timer with resolution better than 1 ms. This was started at the onset of the stimulus and stopped when the button was pressed.

In conventional RT studies, outlier removal is straightforward because conditions, and therefore the shape of the RT histogram, do not change during a run. Because this did not apply here, the following procedure was adopted. Firstly, single RTs which were less than 300 ms or greater than 800 ms were taken to be anticipations or late responses and excluded from further analysis. Regression analysis of RT versus 1/C was performed on the remaining data and the standard error of the $y$ values determined. Outliers from the main distribution were removed by excluding data greater than 1 standard error from the predicted line and the regression repeated. Root-mean-square (RMS) cone contrast was calculated using Judd-transformed $x$, $y$, $L$ values of the ends of the vector and deriving long-, medium-, and short-wavelength cone excitations based on Smith-Pokorny fundamentals (Smith & Pokorny, 1975). Weber contrast was derived for the three cone classes and the RMS calculated. Golz and MacLeod (2003) warn of the pitfalls of using CIE $x$, $y$, and $L$ to compute cone contrast. We have also performed the computation using the phosphors' spectral power distributions and found the errors to be less than 0.5 dB. Multiplying the slope by the RMS cone contrast at maximum modulation gave the slope of the function in terms of cone contrast; RT gain was taken as the reciprocal of this value.

Subjects were three color-normal males with corrected monocular visual acuity of better than 6/6, aged 47 (NRAP), 35 (DM), and 32 (SP) years.

## Results

### Rapid determination of RT gain

The rapid RT gain procedure is depicted in Fig. 1. We have provided this run as an example because it contains some modest
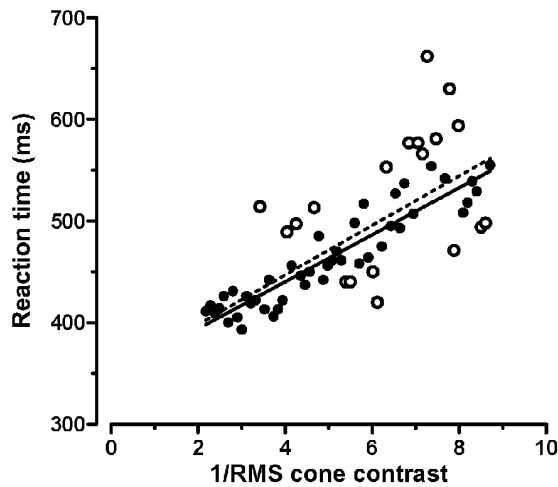
**Fig. 1.** Rapid technique for determining RT gain for an isoluminant gaussian spot, S.D. 0.5 deg, cardinal axis 90 deg, mean luminance 12.5 cd.m$^{-2}$. 1/(RMS cone contrast) was altered in 64 steps of 0.1037 from the maximum (2.178) to close to threshold (8.712). A single RT was recorded to each contrast; values less than 300 or greater than 800 were excluded. The dotted line is the regression line through all remaining data points (open and filled symbols). A new regression line (solid) was computed for all points lying within 1 S.E (on the *y*-axis) of the first line (filled symbols). Open symbols depict data points lying outside this range. RT gain was computed as the reciprocal of the slope of the new line ($k$). In this case, $k$ = 23.13 and RT gain = 0.043. Subject SP.
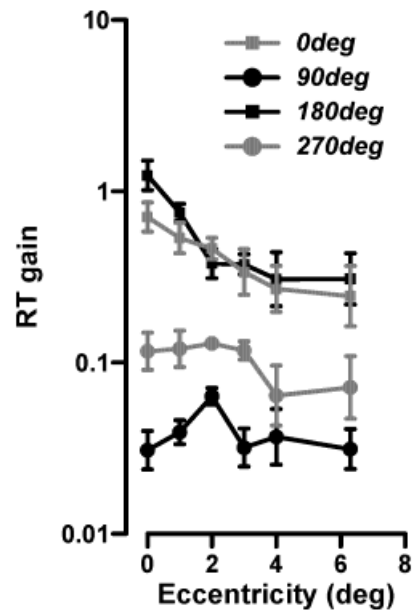


**Fig. 2.** RT gain as a function of eccentricity for the four cardinal axes. The gaussian stimulus, S.D. 0.5 deg, was placed 0, 1, 2, 3, 4, and 6.3 deg to the right of the fixation mark. RT gain was derived using the method illustrated in Fig. 1. Each data point is the mean of three subjects, ±1 S.E.

outliers. RT is plotted as a function of the reciprocal of RMS cone contrast for an isoluminant blue Gaussian spot (90-deg cardinal axis). The slope ($k$) of this function is 23.13. Deriving the same function using the technique described previously (McKeefry et al., 2003) gave a $k$ of 26.25. Thus, the two measures of gain were within 0.005 log units of each other. A similarly close relationship has been found between the two techniques for a wide variety of stimuli. The procedure is complete within about 3 min, in comparison to 30–40 min for the slow technique. Thus, many conditions can be tested in a single experimental session.

*RT gain as a function of cardinal axis and eccentricity*

Fig. 2 depicts the effect of increasing eccentricity (from 0 deg to 6.3 deg) on RT gain using the four cardinal axes and a Gaussian spot with S.D. of 0.5 deg. There is a marked difference between the 0/180-deg and the 90/270-deg data. Gain for the red–green system peaks centrally and falls by about 0.5 log units over the central 4 deg, appearing to flatten off somewhat beyond this. This may reflect localized differences in photoreceptor density—in control studies we have employed L-cone and M-cone isolating stimuli and these have produced gain functions showing a similar distribution (see Discussion). The blue–yellow system does not show this marked central increase in gain. Indeed, for the blue (90 deg) stimulus, gain appears to fall over the central 2-deg eccentricity. The 270-deg data have intermediate values. The data in Fig. 2 are the mean of the three observers, but the same pattern was seen in all three sets of results, notably the peak in the 90-deg function at 2-deg eccentricity.

*Foveal tritanopia*

To explore the possibility that the central lack of S-cones may have played a role in the central dip, we employed a disk-shaped

stimulus with a radius of 0.3 deg, corresponding to the extent of foveal tritanopia (Curcio et al., 1991). To reduce edge effects, a raised cosinusoidal skirt of 0.6 deg in diameter surrounded the disk. The stimulus vector was rotated in small (2 deg) increments in CIE space and thresholds determined for each new vector. The CIE coordinates for 100% modulation along each vector are depicted in Fig. 3a, along with those for each stimulus at threshold.

It can be seen that there is a drop in sensitivity of 50% in terms of vector length as the stimulus vector is rotated from 90 deg to 98 deg. This corresponds to a drop in RMS cone contrast of 49%. The most plausible explanation for this is the paucity of S-cones in this area, revealed by aligning the vector with a tritan confusion line. To check that this is the case, we repeated the experiment for the opposite (270 deg) vector, and for two new white points, one with CIE chromaticity coordinates of $x$ = 0.265 and $y$ = 0.337, and the other of $x$ = 0.346 and $y$ = 0.299. The results are shown in Fig. 3b, in which the resultant vectors converge near to the blue co-punctal point, which has $x$, $y$ coordinates of 0.175 and 0 (Smith & Pokorny, 1975). Because 2-deg increments were used, there is a possible error of about 0.02 along this section of the *x*-axis. Therefore, it is not clear whether there is any significance in the apparent displacement of the vectors in the "away from blue" and the "towards blue" conditions.

Using the same series of vector rotations, we computed RT gain for the white-to-90 deg and white-to-270 deg stimuli. The results are depicted in Fig. 4a. In both blue and yellow directions there was a marked reduction in gain, corresponding in each case to the direction producing the longest vector (see Fig. 3a). For this subject there appears to be a small subsidiary increase in the center of the yellow dip but this is of doubtful significance. The experiment was repeated in the blue direction for larger stimuli, with disk diameters of 0.6 deg and 0.9 deg. These new functions are also plotted in Fig. 4a. As disk diameter increases, so overall gain increases, in agreement with the pooling characteristics of retinal
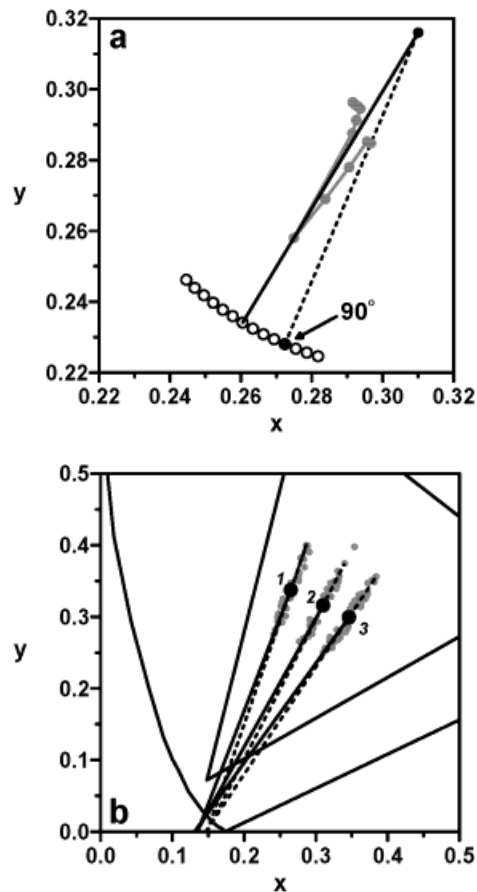
**Fig. 3.** (a) Detection threshold for a stimulus whose vector was rotated away from cardinal 90 deg in 2-deg steps. Each open symbol represents the end point (i.e. maximum modulation) of one of the vectors. Results are plotted in terms of the CIE $x$, $y$ coordinates of the stimulus at threshold. The starting vector is plotted as a dotted line, with black symbols, and the vector with the lowest sensitivity as a solid line. Grey symbols depict the length of the vector at threshold. All vectors originated at $x$, $y$ = 0.31, 0.316. Subject DM. (b) Section of the CIE (1931) chromaticity diagram depicting the results of six similar vector rotation experiments in which the origin's coordinates (black symbols) were (1) $x$ = 0.265, $y$ = 0.337, (2) $x$ = 0.31, $y$ = 0.316, or (3) $x$ = 0.346, $y$ = 0.299. Vectors were extended towards and away from blue. Solid lines depict the resultant vectors for the "towards blue" conditions, and dotted lines the "away from blue" conditions. Grey symbols depict the length of each vector at threshold. Parts of the spectrum locus, the alychne and the monitor gamut, are also visible. Subject DM.

photoreceptors (Metha & Lennie, 2001). However, the effect of vector rotation reduces so that for the largest disk there is no apparent dip. Finally, Figs. 4b and 4c show the effect of vector rotation on the 90-deg and 270-deg eccentricity functions, using the small disk stimulus. Vector rotation such that the stimuli lay along a tritan confusion line emphasizes the central dip and produces about a 1 log-unit reduction in sensitivity between 3–4 deg eccentricity and 0-deg eccentricity. The peak in sensitivity is at a greater eccentricity than in Fig. 2 where, for all three subjects, the 90-deg response peaked at 2-deg eccentricity. It seems plausible that, for the larger (0.5-deg Gaussian) stimulus, there may be contamination from the L-M opponent mechanism, especially when the stimuli are not optimized to fall along a tritan vector.
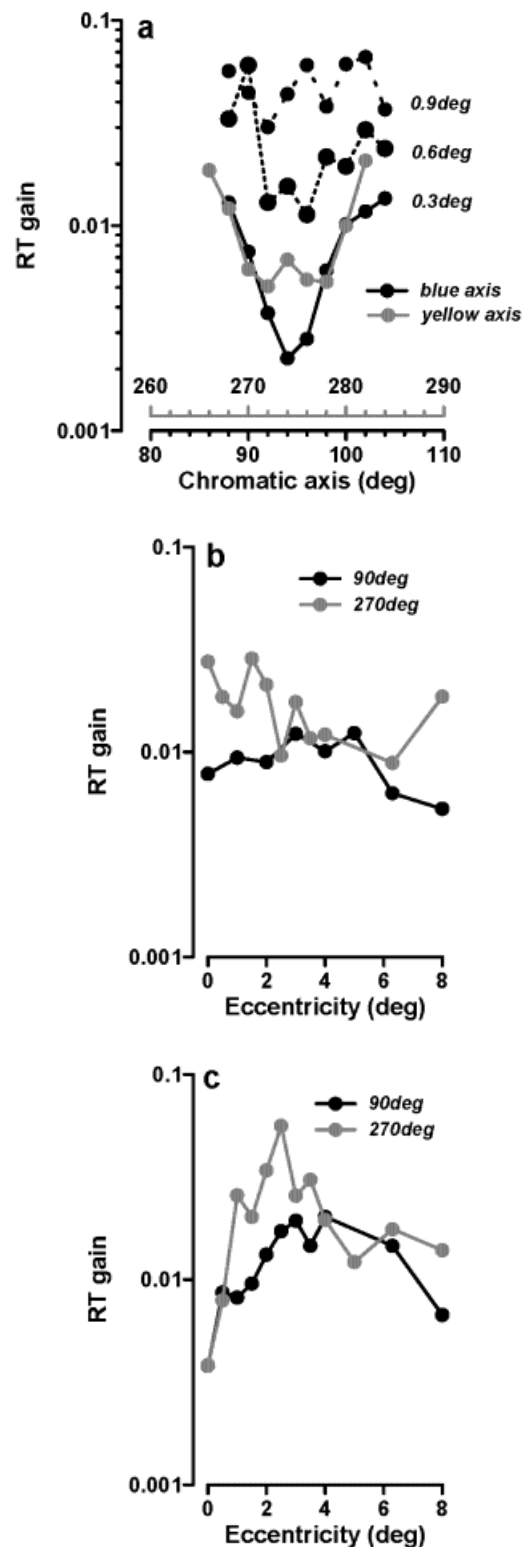
**Fig. 4.** (a) RT gain plotted as a function of vector rotation for white to blue and white to yellow vectors, and a 0.3-deg blurred disk (solid lines— black = 90 deg, grey = 270 deg). Blue data are also depicted for larger disks (0.6 deg and 0.9 deg). In each case, the disk was surrounded by a raised cosinusoidal skirt of twice the diameter. Subject DM. (b) RT gain as a function of eccentricity for 90- and 270-deg cardinal axes and a 0.3-deg blurred disk. Subject DM. (c) RT gain as a function of eccentricity using axes that have been rotated away from 90 deg or 270 deg so that central sensitivity is minimized. 0.3-deg blurred disk. Subject DM.

Thus, the distribution seen in Fig. 4c may provide the most accurate representation of S-cone mediated sensitivity as a function of eccentricity.

## Discussion

We have previously showed a marked difference in RT gain with stimulus vector in isoluminant colour space (McKeefry et al., 2003). That study employed a small Gaussian spot with a S.D. = 0.2 deg, and it is possible that the reduction in sensitivity using the 90- and 270-deg vectors was due to photoreceptor inhomogeneity, in particular the central paucity of S-cones. To investigate this, we took as our starting point a larger stimulus (S.D. = 0.5 deg). We show that careful determination of the tritan line produces a dramatic reduction in gain but that, with these still rather small stimuli, sensitivity is low even if the vectors are not rotated away from the basic 90-deg and 270-deg cardinal axes.

Other psychophysical studies have also examined how chromatic vision changes as a function of retinal eccentricity. A recent study measured cone contrast sensitivities for red–green and blue–yellow sinusoidal gratings between 0 deg and 25 deg of retinal eccentricity (Mullen & Kingdom, 2002). Consistent with this and earlier studies (Anderson et al., 1991; Mullen, 1991), they found that the fovea showed a high degree of specialization for red–green vision, whilst the blue–yellow function varied relatively little across the visual field. Their study used elongated grating patterns and this limited the resolution to steps of 5 deg. Our data fall within their first two steps (0–5 deg and 5–10 deg) and suggest that there may be a peak in blue–yellow opponency between 2-deg and 5-deg eccentricity. Thus, the largest disparity between red–green and blue–yellow gain is seen in the central retina.

One of the limiting factors for cone opponency has to be the retinal distribution of the cones themselves. The 0-deg and 180-deg responses are mediated by L versus M contrast and are thus likely to reflect L- and M-cone activity. The change in gain with eccentricity suggests that sensitivity of the opponent mechanisms, and possibly their underlying cell density, peaks centrally, and this is certainly what anatomical studies show (e.g. Curcio et al., 1990). Elsewhere in this volume our group describes an electroretinogram (ERG) correlate with this observation (Murray et al., 2004). To link these two studies together, we have also used silent substitution and a small disk stimulus to produce L-only and M-only sensitivity versus eccentricity functions. These are remarkably similar to the data illustrated in Fig. 2.

Turning now to the S-cones, Curcio et al. (1991) documented the extent of the S-cone free zone (about 0.35 deg), and suggested that their peak density was at around 1-deg eccentricity. This is borne out by psychophysical studies, in terms of the extent of small-field tritanopia (Williams et al., 1981) and the peak sensitivity of the S-cones (Castano & Sperling, 1982). Our data suggest that the gain of the blue–yellow opponent systems peaks at a somewhat greater eccentricity, which may be the outcome of postreceptoral eccentricity-dependent pooling of the signals (Metha & Lennie, 2001; Calkins, 2001). It is tempting to speculate that this may also be the reason for the absolute difference between the 90-deg and 270-deg data. More recently, Williams' group have produced directly visible evidence in the living human retina using adaptive optics (Roorda & Williams, 1999) and this technique would allow us to correlate anatomy and psychophysics in the same individual. It is apparent from the adaptive optics studies that, unlike the extrafoveal S-cones, L- and M-cone distributions are remarkably inhomogeneous, and

this may have a particular bearing on studies such as ours where the stimulus was quite small.

The presence of macular pigment (MP) in the central 6 deg will have affected the findings and the extent of such effects is addressed in a separate study. Briefly, the peak spectral sensitivity of the S-cones (about 430 nm) is displaced by about 30 nm from the peak absorbance of MP (about 460 nm). Macular pigmentation influences S-cone and M-cone excitation and the strength of this effect is related to its optical density, which can vary dramatically between individuals. Along with other preretinal filtering in the ocular media (in particular lens yellowing), this is responsible for shifting the tritan confusion axis, and is the main factor in interindividual variation in the tritan line. Fig. 3 reveals how sensitive our technique is to small rotations in the tritan line, and it may be used as a convenient method for precisely identifying an individual's tritan axis. Note that Smithson et al. (2003) have described a technique for determining the tritan line. They show how stimulus size and location in the visual field (and therefore macular pigment) can influence the obtained axis in a similar fashion to the findings in Fig. 4.

An additional point concerns the spatial distribution of the MP. Although MP optical density is maximal in the fovea, its effect on our small centrally fixated stimulus may be reduced as there is a very small region over the central foveola where, due to the anatomical distribution of MP in the fibers of Henle, MP is absent (Snodderly et al., 1984). A further issue is the precise optical density spectrum of the MP, which remains in doubt, particularly for the short-wave region of the spectrum. Sharpe et al. (1998) measured central and peripheral spectral sensitivity in deuteranopic, protanopic, and normal observers in order to test the assumptions on which MP optical density spectrum estimations are based. They speculated that estimates of MP optical density spectra might be influenced by local variations in the optical density of the cone pigments not previously observed.

In conclusion, the variation in RT contrast gain as a function of retinal eccentricity relates closely to the variation in the L-, M-, and S-cone photoreceptor densities and reveals that inhomogeneities in their retinal distribution can have marked effects on RTs. Along with macular pigment variations, this is likely to be a major contributory factor to previously reported differences in RT to small stimuli of varying chromaticity.

## References

ANDERSON, S.J., MULLEN, K.T. & HESS, R.F. (1991). Human peripheral spatial resolution for achromatic and chromatic stimuli—limits imposed by optical and retinal factors. *Journal of Physiology* (London) **442**, 47–64.

CALKINS, D.J. (2001). Seeing with S cones. *Progress in Retinal and Eye Research* **20**, 255–287.

CASTANO, J.A. & SPERLING, H.G. (1982). Sensitivity of the blue-sensitive cones across the central retina. *Vision Research* **22**, 661–673.

CURCIO, C.A., SLOAN, K.R., KALINA, R.E. & HENDRICKSON, A.E. (1990). Human photoreceptor topography. *Journal of Comparative Neurology* **292**, 497–523.

CURCIO, C.A., ALLEN, K.A., SLOAN, K.R., LEREA, C.L., HURLEY, J.B., KLOCK, I.B. & MILAM, A.H. (1991). Distribution and morphology of human cone photoreceptors stained with anti-blue opsin. *Journal of Comparative Neurology* **312**, 610–624.

DERRINGTON, A.M., KRAUSKOPF, J. & LENNIE, P. (1984). Chromatic mechanisms in lateral geniculate nucleus of macaque. *Journal of Physiology* (London) **357**, 241–265.

GOLZ, J. & MACLEOD, D.I.A. (2003). Colorimetry for CRT displays. *Journal of the Optical Society of America A* **20**, 769–781.

MACLEOD, D.I.A. & BOYNTON, R.M. (1979). Chromaticity diagram show-

ing cone excitation by stimuli of equal luminance. *Journal of the Optical Society of America* **69**, 1183

McKeefry, D.J., Parry, N.R.A. & Murray, I.J. (2003). Simple reaction times in colour space: The influence of chromaticity, contrast and cone opponency. *Investigative Ophthalmology and Visual Science* **44**, 2267–2276.

Metha, A.B. & Lennie, P. (2001). Transmission of spatial information in S-cone pathways. *Visual Neuroscience* **18**, 961–972.

Mullen, K.T. (1991). Color vision as a post-receptoral specialization of the central visual field. *Vision Research* **31**, 119–130.

Mullen, K.T. & Kingdom, F.A.A. (2002). Differential distributions of red–green and blue–yellow cone opponency across the visual field. *Visual Neuroscience* **19**, 109–118.

Murray, I.J., Parry, N.R.A., Kremers, J., Stepien, M. & Schild, A. (2004). Photoreceptor topography and cone-specific ERGs. *Visual Neuroscience* **21**, 231–235.

Murray, I.J. & Plainis, S. (2003). Contrast coding and magno/parvo segregation revealed in reaction time studies. *Vision Research* **43**, 2707–2719.

Plainis, S. & Murray, I.J. (2000). Neurophysiological interpretation of human visual reaction times: Effect of contrast, spatial frequency and luminance. *Neuropsychologia* **38**, 1555–1564.

Roorda, A. & Williams, D.R. (1999). The arrangement of the three cone classes in the living human eye. *Nature* **397**, 520–522.

Sharpe, L.T., Stockman, A., Knau, H. & Jagle, H. (1998). Macular pigment densities derived from central and peripheral spectral sensitivity differences. *Vision Research* **38**, 3233–3239.

Smith, V.C. & Pokorny, J. (1975). Spectral sensitivity of the foveal cone photopigment between 400 and 500 nm. *Vision Research* **15**, 161–171.

Smithson, H.E. & Mollon, J.D. (2001). Reaction times to brief chromatic stimuli. *Investigative Ophthalmology and Visual Science* **42**, 532.

Smithson, H.E., Sumner, P. & Mollon, J.D. (2003). How to find a Tritan line. In *Normal and Defective Colour Vision*, ed. Mollon, J.D., Pokorny, J. & Knoblauch, K., pp. 279–287. New York: Oxford University Press.

Snodderly, D.M., Brown, P.K., Delori, F.C. & Auran, J.D. (1984). The macular pigment, 1. Absorbance spectra, localization, and discrimination from other yellow pigments in primate retinas. *Investigative Ophthalmology and Visual Science* **25**, 660–673.

Williams, D.R., MacLeod, D.I.A. & Hayhoe, M.M. (1981). Foveal Tritanopia. *Vision Research* **21**, 1341–1356.